Published in final edited form as:
Gastroenterology. 2012 March ; 142(3): 612–621.e5. doi:10.1053/j.gastro.2011.11.029.

Fibromodulin, an Oxidative Stress-Sensitive Proteoglycan, Regulates the Fibrogenic Response to Liver Injury in Mice

Elisabetta Mormone[*], **Yongke Lu**[*], **Xiaodong Ge**[*], **Maria Isabel Fiel**[‡], and **Natalia Nieto**[*]

[*]Division of Liver Diseases, Department of Medicine, Mount Sinai School of Medicine, New York, New York

[‡]Division of Liver Diseases, Department of Pathology, Mount Sinai School of Medicine, New York, New York

Abstract

BACKGROUND & AIMS—Collagen I deposition contributes to liver fibrosis, yet little is known about other factors that mediate this process. Fibromodulin is a liver proteoglycan that regulates extracellular matrix organization and is induced by fibrogenic stimuli. We propose that fibromodulin contributes to the pathogenesis of fibrosis by regulating the fibrogenic phenotype of hepatic stellate cells (HSCs).

METHODS—We analyzed liver samples from patients with hepatitis C–associated cirrhosis and healthy individuals (controls). We used a coculture model to study interactions among rat HSCs, hepatocytes, and sinusoidal endothelial cells. We induced fibrosis in livers of wild-type and *Fmod*$^{-/-}$ mice by bile duct ligation, injection of CCl_4, or administration of thioacetamide.

RESULTS—Liver samples from patients with cirrhosis had higher levels of *fibromodulin* messenger RNA and protein than controls. Bile duct ligation, CCl_4, and thioacetamide each increased levels of fibromodulin protein in wild-type mice. HSCs, hepatocytes, and sinusoidal endothelial cells produced and secreted fibromodulin. Infection of HSCs with an adenovirus that expressed fibromodulin increased expression of collagen I and α–smooth muscle actin, indicating increased activation of HSCs and fibrogenic potential. Recombinant fibromodulin promoted proliferation, migration, and invasion of HSCs, contributing to their fibrogenic activity. Fibromodulin was sensitive to reactive oxygen species. HepG2 cells that express cytochrome P450 2E1 produced fibromodulin, and HSCs increased fibromodulin production in response to pro-oxidants. In mice, administration of an antioxidant prevented the increase in fibromodulin in response to CCl_4. Coculture of hepatocytes or sinusoidal endothelial cells with HSCs increased the levels of reactive oxygen species in the culture medium, along with collagen I and fibromodulin proteins; this increase was prevented by catalase. Fibromodulin bound to collagen I, but the binding did not prevent collagen I degradation by matrix metalloproteinase 13. Bile duct ligation caused liver fibrosis in wild-type but not *Fmod*$^{-/-}$ mice.

Reprint requests. Address requests for reprints to: Natalia Nieto, PhD, Division of Liver Diseases, Department of Medicine, Mount Sinai School of Medicine, Box 1123, 1425 Madison Avenue, Room 11-70, New York, New York 10029. natalia.nieto@mssm.edu; fax: (212) 849-2574.
E.M. and Y.L. contributed equally to this work.

Supplementary Material

Note: To access the supplementary material accompanying this article, visit the online version of *Gastroenterology* at www.gastrojournal.org, and at doi: 10.1053/j.gastro.2011.11.029.

Conflicts of interest
The authors disclose no conflicts.

CONCLUSIONS—Fibromodulin levels are increased in livers of patients with cirrhosis. Hepatic fibromodulin activates HSCs and promotes collagen I deposition, which leads to liver fibrosis in mice.

Keywords

Mouse Model; Liver Disease; Intercellular Communication; Fibers

Although different cell types contribute to the increase in fibrillar collagen I levels during hepatic fibrogenesis, they all undergo a common process of differentiation and acquisition of a classic myofibroblast-like phenotype. Portal fibroblasts play a significant role in the development of portal fibrosis; however, hepatic stellate cells (HSCs) play a major role in collagen I deposition when hepatocellular injury is concentrated within the liver lobule and sinusoids.

Efforts to understand the pathogenesis of liver fibrosis focus on events that lead to the activation of profibrogenic cells and to early accumulation of scar (ie, fibrillar collagen I) to identify therapeutic targets to prevent its onset, slow its progression, or help its resolution.[1] Stimuli initiating activation, proliferation, migration, and invasion of HSCs derive from injured hepatocytes,[2,3] Kupffer cells,[4,5] sinusoidal endothelial cells (SECs),[6] and inflammatory cells[7] in addition to rapid changes in extracellular matrix (ECM) composition.[1]

Synthesis of collagen I is regulated by the ECM itself, and even though the basement membrane matrix preserves quiescence of HSCs, collagen I further enhances HSC activation in a paracrine manner. Increasingly, reactive oxygen species (ROS) are viewed as candidate drivers of HSC activation and collagen I up-regulation[3,4,8,9]; however, downstream mediators for the ROS effects on the activation of HSCs and the increase in collagen I levels require further study.

Synthesis and secretion of collagen I are a major focus of interest, during the onset of liver fibrosis; nevertheless, there is also considerable deposition of proteoglycans, glycoproteins, and glycosaminglycans into the space of Disse.[10] Fibromodulin (FMOD) is a small leucine-rich proteoglycan regulating ECM organization, which has been described as essential for tissue repair in multiple organs.[11] This family of proteoglycans is involved in cell metabolism via binding to growth factors as well as in matrix organization by interacting with various collagens.[12–15] *Fmod*$^{-/-}$ mice develop abnormal collagen fibril architecture in connective tissues in addition to showing increased age-dependent osteoarthritis and degenerative changes in cartilage structure[14,16,17]; thus, FMOD plays a significant role in defining tissue integrity.[14] Moreover, in vivo both collagen and FMOD are likely to have an important functional role in tissues where they are coexpressed due to potential physical interaction between both proteins.[18]

Thus far, there is no information on whether FMOD is present in the liver, which cells express it, and where specifically it is induced upon the establishment of hepatic injury.[19] In addition, little is known about its potential role in the development of liver fibrosis,[19] whether induction of FMOD in liver cells could contribute to the profibrogenic potential of HSCs, and the molecular mechanism involved in these events.

Identifying if FMOD stimulates the profibrogenic response to hepatic damage could be central for understanding the pathogenesis of liver fibrosis. Thus, the aim of this study was to explore how FMOD regulates the HSC profibrogenic phenotype, a key event in liver fibrosis, as well as the consequences of in vivo ablation of the *Fmod* gene for the fibrogenic response to liver injury under a profibrogenic stimuli. To investigate this, we used a co-

culture model that resembles aspects of the interplay between liver cells in addition to inducing liver fibrosis in vivo using wild-type (WT) and *Fmod*$^{-/-}$ mice. The results suggest that hepatic FMOD, sensitive to oxidant stress, contributes to HSC activation and collagen I deposition, thus participating in the pathogenesis of liver fibrosis.

Materials and Methods

Cell Treatments

Rat HSCs (250,000 cells/well) were seeded on 6-well plates in Dulbecco's modified Eagle medium/F12 with 10% fetal bovine serum. Primary cells were cultured using Dulbecco's modified Eagle medium/F12 for 4 to 7 days, which was replaced by serum-deprived Dulbecco's modified Eagle medium/F12 before treatment with 50 nmol/L endotoxin-free human recombinant FMOD (rFMOD) for 24 hours (donated by Dr Ake Oldberg, Lund University, Lund, Sweden). Cells were infected with Ad-LUC or Ad-FMOD at a multiplicity of infection of 50 for 48 hours. The adenoviruses were a gift from Dr David T. Curiel (Washington University, St Louis, MO). H_2O^2 (25 μmol/L) and catalase (200 U/mL) were added to the cells for 24 hours (both from Sigma, St Louis, MO).

Mice

Fmod$^{-/-}$ mice and their WT littermates (C57BL/6J) were obtained from Dr Marian Young (National Institutes of Health, Bethesda, MD).[20,21] These mice were backcrossed for at least 10 generations. Colonies were established by intercrossing *Fmod*$^{+/-}$ mice, and littermates were used in all experiments. *Fmod*$^{-/-}$ mice have normal heart, liver, lung, skin, and cartilage; however, they show abnormal tissue organization, collagen fiber bundles, and fiber architecture.[22]

Induction of Liver Injury

Ten-week-old male WT mice and their *Fmod*$^{-/-}$ littermates were used in all experiments. To induce liver injury, 3 in vivo models were used. In the first model, cholestasis was induced by placing a ligature around the common bile duct while controls were sham operated. All mice were killed 3 weeks later. In the second model, mice were intraperitoneally injected twice a week with 0.5 mL/kg body wt CCl_4 (Sigma) or an equal volume of mineral oil for 1 month and killed 48 hours after the last injection of CCl_4. In the third model, mice were treated with thioacetamide (TAA) (300 mg/L; Sigma) in the drinking water or received an equal volume of water for 4 months. Mice were killed 48 hours after withdrawal of TAA. Blood was collected by orbital venous plexus bleeding. Each liver was excised into fragments by using the same liver lobe for biochemical assays and paraffin embedding for staining. All animals received humane care according to the criteria outlined in the Guide for the Care and Use of Laboratory Animals prepared by the National Academy of Sciences and published by the National Institutes of Health.

Human Samples

Dr Andrea D. Branch (Mount Sinai School of Medicine, New York, NY) provided the human liver protein lysates and RNA from resections from de-identified controls and subjects with biopsy-proven stage 3 hepatitis C virus (HCV) cirrhosis. Samples were scored according to the Scheuer/Ludwig Batts classification.[23,24] These samples were exempt from institutional review board approval because no patient information was disclosed.

Pathology

In all experiments, the left liver lobe was excised and fixed in 10% neutral-buffered formalin and processed into paraffin sections for H&E or immunohistochemistry (IHC) and scoring

by the Brunt classification. Portal and lobular inflammation were noted to be lymphocytes present in the lobules or portal areas and were scored as follows: 1 = rare foci; 2 = up to 5 foci; 3 = >5 foci. Centrilobular necrosis and parenchymal necrosis were each separately scored. The scores for centrilobular necrosis were as follows: 1 = hepatocyte necrosis affecting only zone 3; 2 = in addition to zone 3 necrosis, occasional bridging necrosis was seen; 3 = pronounced bridging and confluent necrosis. Parenchymal necrosis was noted to be spotty necrosis or apoptosis in zones 2 and 1. The scores for parenchymal necrosis were as follows: 1 = ≤1 focus; 2 = 5–10 foci; 3 = ≥10 foci at 100×. Ductular reaction was noted to be proliferation of bile ductules at the margins of the portal tracts, and the score was as follows: 1 = rare bile ductules present; 2 = irregular buds of bile ductules affecting some portal tracts; 3 = when bile ductules are more prominent and affect the majority of portal areas and/or strings of bile ductular epithelial cells were seen intermingled with hepatocytes. The degree of fibrosis ranged from 0 to 4 and was patterned after the Brunt system.[25] Briefly, this was as follows: 1 = perisinusoidal/perivenular fibrosis alone; 2 = 1 plus portal fibrosis; 3 = bridging fibrosis; 4 = cirrhosis. The assessment of the preceding scores was uniformly performed under 100× magnification in 10 fields per sample and twice.

Immunohistochemistry

The collagen I antibody used on IHC was from Millipore (Billerica, MA), the FMOD and cytokeratin-19 antibodies were from Santa Cruz Biotechnology (Santa Cruz, CA), the α–smooth muscle actin (α-SMA) antibody was from Sigma, and the desmin antibody was from Dako (Carpinteria, CA). The FMOD antibody was tested in livers from *Fmod*$^{-/-}$ mice and competed with rFMOD (2.5 μg rFMOD and 2 μg FMOD antibody in 1 mL were incubated for 30 min at room temperature) to ensure specificity (Supplementary Figure 1). Reactions were developed using the Histostain Plus Detection System (Invitrogen, Carlsbad, CA). For the Sirius red computer-assisted morphometry assessment, the integrated optical density was calculated from 10 random fields per sample containing similar-size portal tract or hepatic vein at 100× and using Image-Pro 7.0 Software (Media Cybernetics, Bethesda, MD). The results were averaged and expressed as fold change over controls.

Statistical Analysis

Data were analyzed by a 2-factor analysis of variance, and results are expressed as mean ± SEM. All in vitro experiments were performed in triplicate at least 4 times. A representative blot is shown in all figures. Eight mice per group were used in all the in vivo experiments, which were repeated twice.

Results

FMOD Increases in Patients With Stage 3 HCV-Induced Cirrhosis

To determine whether FMOD is expressed in human livers, resections from healthy patients and patients with biopsy-proven stage 3 HCV-induced cirrhosis were studied for FMOD protein and messenger RNA (mRNA) expression. Western blot analysis showed an increase in both FMOD and collagen I protein levels in patients with HCV-induced cirrhosis compared with healthy explants (Figure 1*A*). Likewise, there was an 8-fold increase in *FMOD* mRNA levels in patients with HCV-induced cirrhosis compared with healthy explants (Figure 1*B*). Hence, these results confirm that FMOD is expressed in human liver and that it is up-regulated in stage 3 HCV-induced cirrhosis.

Expression of FMOD Is Up-regulated in Cholestasis and in Drug-Induced Liver Injury in Mice

To dissect if FMOD also increased during liver injury in mice, we used well-established in vivo models of liver fibrosis such as common bile duct ligation (BDL), which causes cholestatic liver damage, or long-term CCl_4 injection and TAA treatment to provoke drug-induced liver injury. These 2 drugs undergo cytochrome P450 metabolism, leading to significant oxidant stress, inflammation, and pericentral necrosis.

FMOD protein was induced under chronic common BDL (Figure 2*A*), CCl_4 injection (Figure 2*B*), and TAA treatment (Figure 2*C*). In all 3 models, FMOD expression was detected mostly in the sinusoids and in hepatocytes. FMOD protein expression in the BDL, CCl_4, and TAA models was also validated by Western blot analysis (Figure 2*D*). Thus, there was an association between FMOD protein up-regulation and the extent of liver injury in mice.

To identify the specific cell type that expressed FMOD, chronic CCl_4-injured WT mouse livers were perfused and primary cells were isolated. Western blot analysis revealed that HSCs, hepatocytes, and SECs expressed and secreted FMOD protein (Figure 2*E* and *F*); however, Kupffer cells did not express FMOD (not shown).

FMOD Activates and Induces Profibrogenic Effects in HSCs

Because FMOD protein was found induced in HSCs during liver injury, we hypothesized that endogenous FMOD could enhance activation of HSCs and their profibrogenic potential. To show this, rat HSCs were infected with Ad-LUC or Ad-FMOD. Adenoviral infection did not alter HSC viability or phenotype (Figure 3*A*, *left*). Along with enhanced intracellular FMOD expression, intracellular collagen I and to some extent α-SMA, a marker of HSC activation, were increased by Ad-FMOD compared with Ad-LUC infection (Figure 3*A*, *right*). Hence, an autocrine role for intracellular FMOD in modulating collagen I deposition and HSC activation could be established.

Because the IHC analysis also identified hepatocytes and SECs as sources of FMOD, and FMOD was secreted by all 3 cell types, next we questioned whether extracellular FMOD could play a role in regulating the profibrogenic phenotype of HSCs, which entails their proliferative, migratory, and invasive potential. To evaluate this, rat HSCs were challenged with rFMOD and cell proliferation, migration, and invasion were evaluated over time. rFMOD induced HSC proliferation by 35%, as shown by the rate of *methyl*[^{3}H]-thymidine incorporation into the DNA of HSCs (Figure 3*B*). Migration, measured by wound closure, was also enhanced by rFMOD treatment (Figure 3*C*, *arrows*), and it was not blocked by preincubation with mitomycin to inhibit mitosis (not shown). Lastly, HSC invasion or chemotaxis was increased by 6-fold in the presence of rFMOD when compared with nontreated cells (Figure 3*D* and *E*). Overall, these findings show that FMOD also exerts a paracrine role in regulating the profibrogenic behavior and phenotype of HSCs.

ROS Increase FMOD Protein Expression

Because cholestasis and drug-induced liver injury generate a significant amount of ROS due to glutathione depletion and increased ROS generation, mostly via cytochrome P450 2E1 activation,[26] next we evaluated whether FMOD was ROS sensitive. First, HepG2 cells overexpressing cytochrome P450 2E1, as a source of ROS, were analyzed for FMOD expression. Western blot analysis showed significant up-regulation of both cytochrome P450 2E1 and intracellular and extracellular FMOD proteins (Figure 4*A*). In addition, primary rat HSCs incubated with H_2O_2 displayed greater intracellular and extracellular FMOD expression than nontreated HSCs (Figure 4*B*).

To validate the induction of FMOD by oxidative stress in vivo, WT mice were injected with CCl_4 for 1 month in the presence or absence of *S*-adenosylmethionine, an antioxidant known to restore glutathione levels, or mineral oil. Coinjection with *S*-adenosylmethionine lowered by 50% FMOD protein levels (Supplementary Figure 2*A*) and the extent of liver fibrosis[27] when compared with mice injected with CCl_4 alone. Overall, these data indicate that FMOD is an ROS-sensitive proteoglycan. Because collagen I is highly inducible by oxidant stress,[28] FMOD could be a potential mediator regulating collagen I deposition.

Hepatocytes and SECs Increase FMOD and Collagen I Levels in HSCs in Coculture

Because in vivo models of cholestasis or drug-induced liver injury identified hepatocytes and SECs as sources of FMOD in addition to HSCs, which were responsive to rFMOD, to analyze whether these cells also contributed to the fibrogenic response in a paracrine fashion, cocultures with HSCs were established. Primary rat HSCs were placed in coculture with either primary SECs or hepatocytes. Coculture with either cell type led to an increase in ROS levels (mostly hydroperoxides) in the cell culture medium compared with HSCs cultured alone. As anticipated, the increase in ROS was rather significant in the hepatocyte coculture compared with the SEC coculture (Figure 5*A*); hence, based on our previous studies showing the effect of hepatocyte-derived ROS generation on the HSC profibrogenic behavior,[9,29–32] we prioritized this coculture model.

Coculture of HSCs with SECs increased both intracellular FMOD and collagen I protein expression compared with the HSC monoculture; however, extracellular FMOD and collagen I were undetectable (Figure 5*B*). In contrast, coculture of HSCs with hepatocytes notably elevated both intracellular and extracellular collagen I and FMOD protein levels when compared with the HSC monoculture (Figure 5*C*). Thus, these results show that FMOD from neighboring cells could also signal to enhance the HSC profibrogenic response.

Lastly, because the coculture of HSCs with hepatocytes showed the highest increase in ROS levels, based on previous work,[9,29–32] to determine whether ROS could be upstream of FMOD, the hepatocyte and HSC coculture was incubated in the presence of an antioxidant. Catalase, which decomposes H_2O_2 and other hydroperoxides, prevented the increase in intracellular and extracellular collagen I as well as in FMOD and α-SMA levels in HSCs cocultured with hepatocytes, suggesting an ROS-dependent mechanism for the profibrogenic effects of FMOD on HSCs (Figure 5*D*).

FMOD Binds Collagen I but Does Not Prevent Collagen I Degradation by Matrix Metalloproteinase 13

Because the interaction between collagen I and FMOD could increase the stability of collagen I, hence favoring scarring, samples from cocultures of HSCs with hepatocytes were immunoprecipitated with anti-FMOD antibody and immunoblotted with anti–collagen I antibody. There was binding of FMOD and collagen I proteins (Supplementary Figure 3*A*). Infection of HSCs with Ad-FMOD to overexpress FMOD and treatment with active matrix metalloproteinase 13, a key HSC protease known to degrade collagen I within the triple-helical structure,[33] did not alter collagen I degradation compared with HSCs infected with Ad-LUC and treated with active matrix metalloproteinase 13 (Supplementary Figure 3*B*). Thus, the FMOD/collagen I binding in HSCs did not increase collagen I stability against matrix metalloproteinase 13 proteolytic degradation.

BDL Induces More Liver Injury and Fibrosis in WT Than in *Fmod*−/− Mice

Because the in vitro data suggested a profibrogenic role for FMOD, next we asked whether complete *Fmod* ablation could confer protection in the chronic BDL model. WT and *Fmod*$^{-/-}$ mice were either bile duct ligated or sham operated and killed 3 weeks later. Serum

γ-glutamyltransferase activity increased in BDL compared with sham-operated WT mice, whereas lower activity was observed in *Fmod*$^{-/-}$ mice (Figure 6*A*). H&E staining showed that coagulative necrosis, inflammation, and ductular reaction were present in BDL WT mice but were less apparent in *Fmod*$^{-/-}$ mice (Figure 6*B*). The scores for necrosis, portal inflammation, lobular inflammation, and ductular reaction validated these findings (Figure 6*C–F*). Lastly, IHC analysis depicted more desmin, collagen I deposition, Sirius red staining and morphometry, cytokeratin-19 (a marker for ductular reaction), and neutrophil staining in BDL WT than in *Fmod*$^{-/-}$ mice (Figure 7*A–E*); however, similar transforming growth factor β expression was detected by Western blot analysis and IHC (not shown) in CCl_4-injected WT and *Fmod*$^{-/-}$ mice (Supplementary Figure 2*B*). Thus, *Fmod* ablation prevented BDL-induced fibrosis in mice.

WT Mice Show More CCl_4-Induced Chronic Liver Injury and Fibrosis Than *Fmod*−/− Mice

To dissect whether *Fmod* ablation could be protective in a model of chronic drug-induced liver injury affecting mostly the central zone, 10-week-old male WT and *Fmod*$^{-/-}$ mice were treated with CCl_4 or mineral oil intraperitoneally for 1 month and were killed 48 hours after the last injection to prevent acute liver injury. H&E staining and pathology scoring according to the Brunt classification, collagen I IHC, Sirius red/fast green staining and morphometry, and α-SMA IHC revealed more inflammation, necrosis, fibrosis, and α-SMA expression in CCl_4-injected WT mice than in *Fmod*$^{-/-}$ mice (Supplementary Figure 4). These results confirm that *Fmod* deletion protects from liver fibrosis.

Discussion

The overall goal of this study was to determine the potential role of FMOD on the profibrogenic phenotype of HSCs and its contribution to the fibrogenic response to liver injury. Although previous work by Krull et al[19] did not identify *Fmod* mRNA in normal rat liver, our studies show that FMOD protein is expressed in human liver and is significantly elevated in patients with stage 3 HCV-induced cirrhosis compared with healthy individuals. Induction of FMOD has been previously described in bleomycin-induced pulmonary fibrosis in rats,[34] and *FMOD* gene transcription is induced by UV irradiation.[35] In addition, we show that FMOD expression is up-regulated in cholestasis in the BDL model and in drug-induced liver injury in the CCl_4 and TAA models in WT mice.

FMOD-positive staining was identified mostly in parenchymal and in sinusoidal areas. Specificity of the FMOD staining on IHC was further confirmed by using *Fmod*$^{-/-}$ mice by competing with rFMOD and by isolating primary cells from CCl_4-treated WT mice. Hepatocytes, SECs, and HSCs, but not Kupffer cells, expressed FMOD protein. Thus, we speculated that the effects of FMOD on HSCs would be both of autocrine and paracrine nature because HSCs were exposed to secreted FMOD produced by themselves and by neighboring liver cells.

To evaluate the autocrine effects of FMOD on the HSC profibrogenic phenotype, intracellular FMOD was induced by infecting HSCs with Ad-FMOD. This resulted in an increase in intracellular and extracellular collagen I along with α-SMA, thus validating an autocrine role for FMOD in driving HSC activation and in promoting their profibrogenic potential.

To dissect whether extracellular FMOD could also condition the HSC behavior, cells were incubated in the presence of rFMOD, which caused an increase in HSC proliferation, migration, and invasive potential. These are important functions gained by HSCs during their activation process and greatly contribute to their profibrogenic ability. Thus, the

experimental data suggest that FMOD activates and induces a profibrogenic response in HSCs in both an autocrine and a paracrine manner.

Oxidative stress represents a common link among different modes of persistent liver injury. Because FMOD is expressed in hepatocytes, SECs, and HSCs and FMOD was found to be ROS sensitive in vitro and in vivo, also described by others in fibroblasts,[36] we speculated that communication between these cell types could lead to an enhanced profibrogenic behavior in HSCs. Several studies, including our own,[3,9,37] have evaluated the role of conditioned medium from hepatocytes and SECs in stimulating HSCs.[31,32] These studies have identified ROS as key mediators for the profibrogenic actions on HSCs.

To date, there is limited information on the specific ROS-sensitive mediators secreted by hepatocytes, SECs, and HSCs, as well as the molecular mechanisms by which these molecules modulate the fibrogenic response in HSCs. Thus, a coculture model was developed to study the role of hepatocytes and SEC-secreted FMOD on HSC activation and collagen I production. These models resemble aspects of the cross talk of hepatocytes and SECs with HSCs in vivo and have been previously used to gain mechanistic insight on the communication between these cell types.[2,3] A novel role of FMOD as an ROS downstream effector on collagen I up-regulation and HSC activation was identified, which was blocked by catalase, an antioxidant.

Thus, FMOD could also convey paracrine-mediated signaling to regulate the profibrogenic behavior of HSCs; however, whether these effects require receptor binding and further intracellular signaling in HSCs still remains to be determined because the FMOD receptors, if any, have not been identified so far. In addition, FMOD did not exert its profibrogenic effects by modulating transforming growth factor β, a well-known profibrogenic factor,[14,38] because Western blot analysis showed similar transforming growth factor β expression in BDL *Fmod*$^{-/-}$ and in WT mice. Our studies also ruled out that the physical interaction between FMOD and collagen I could prevent the matrix metalloproteinase 13–mediated collagen I proteolysis in HSCs, thus contributing to ECM deposition.

All these results suggested that *Fmod* gene ablation could protect from the onset of liver fibrosis. The in vivo data showed that in the chronic BDL model, where significant periportal fibrosis occurs due to biliary hyperplasia, *Fmod*$^{-/-}$ mice developed less coagulative necrosis, inflammation, biliary epithelial cell proliferation, ductular reaction, and neutrophil infiltration than WT mice. Moreover, collagen I expression was lower in BDL *Fmod*$^{-/-}$ compared with WT mice, and comparable findings were obtained in mice treated with CCl_4, which also depicted lower α-SMA induction.

In conclusion, our results identified FMOD as expressed in the liver and induced upon the onset of chronic liver injury. Furthermore, they suggest a role for the ROS-driven FMOD increase in regulating HSC activation and their profibrogenic potential both in an autocrine and a paracrine fashion; hence, FMOD could be considered as a new target to prevent the development and progression of liver fibrosis.

Supplementary Material

Refer to Web version on PubMed Central for supplementary material.

Acknowledgments

The authors thank Dr Andrea D. Branch (Mount Sinai School of Medicine, New York, NY) for providing the human liver protein lysates, Dr Marian Young (National Institutes of Health, Bethesda, MD) for donating the *Fmod*$^{-/-}$ mice, Dr Ake Oldberg (University of Lund, Lund, Sweden) for the rFMOD, Dr David T. Curiel

(Washington University, St Louis, MO) for the Ad-FMOD, and Dr Arthur I. Cederbaum (Mount Sinai School of Medicine, New York, NY) for providing the HepG2 cells overexpressing cytochrome P450 2E1; the following members of the Nieto Laboratory: Dr Raquel Urtasun for facilitating the samples from the CCl_4-injected WT mice, Dr Xiaodong Wang for providing the samples from the TAA-treated WT mice and for technical assistance in setting up the conditions for IHC, and Drs Aritz Lopategi and Tung Ming Leung for their technical help during the BDL and CCl_4 models as well as the cell invasion assays; and all the past and current members of the Nieto Laboratory for their helpful discussions and valuable insight throughout the course of this project.

Funding

Supported by US Public Health Service grants 5R01 DK069286 and 2R56 DK069286 from the National Institute of Diabetes and Digestive and Kidney Diseases and 5P20 AA017067 and 5P20 AA017067-03S1 from the National Institute on Alcohol Abuse and Alcoholism (to N.N.).

Abbreviations used in this paper

α;-SMA	α;–smooth muscle actin
BDL	bile duct ligation
ECM	extracellular matrix
FMOD	fibromodulin
HSC	hepatic stellate cell
IHC	immunohistochemistry
rFMOD	recombinant fibromodulin
ROS	reactive oxygen species
SEC	sinusoidal endothelial cell
TAA	thioacetamide
WT	wild-type

References

1. Friedman SL. Molecular regulation of hepatic fibrosis, an integrated cellular response to tissue injury. J Biol Chem. 2000; 275:2247–2250. [PubMed: 10644669]
2. Nieto N, Cederbaum AI. Increased Sp1-dependent transactivation of the LAMgamma 1 promoter in hepatic stellate cells co-cultured with HepG2 cells overexpressing cytochrome P450 2E1. J Biol Chem. 2003; 278:15360–15372. [PubMed: 12529372]
3. Nieto N, Friedman SL, Cederbaum AI. Cytochrome P450 2E1-derived reactive oxygen species mediate paracrine stimulation of collagen I protein synthesis by hepatic stellate cells. J Biol Chem. 2002; 277:9853–9864. [PubMed: 11782477]
4. Nieto N. Oxidative-stress and IL-6 mediate the fibrogenic effects of rodent Kupffer cells on stellate cells. Hepatology. 2006; 44:1487–1501. [PubMed: 17133487]
5. Cubero FJ, Nieto N. Ethanol and arachidonic acid synergize to activate Kupffer cells and modulate the fibrogenic response via tumor necrosis factor alpha, reduced glutathione, and transforming growth factor beta-dependent mechanisms. Hepatology. 2008; 48:2027–2039. [PubMed: 19003881]
6. Wirz W, Antoine M, Tag CG, et al. Hepatic stellate cells display a functional vascular smooth muscle cell phenotype in a three-dimensional co-culture model with endothelial cells. Differentiation. 2008; 76:784–794. [PubMed: 18177423]
7. Casini A, Ceni E, Salzano R, et al. Neutrophil-derived superoxide anion induces lipid peroxidation and stimulates collagen synthesis in human hepatic stellate cells: role of nitric oxide. Hepatology. 1997; 25:361–367. [PubMed: 9021948]
8. Novo E, Busletta C, Bonzo LV, et al. Intracellular reactive oxygen species are required for directional migration of resident and bone marrow-derived hepatic pro-fibrogenic cells. J Hepatol. 2011; 54:964–974. [PubMed: 21145826]

9. Nieto N, Friedman SL, Cederbaum AI. Stimulation and proliferation of primary rat hepatic stellate cells by cytochrome P450 2E1-derived reactive oxygen species. Hepatology. 2002; 35:62–73. [PubMed: 11786960]
10. Hogemann B, Edel G, Schwarz K, et al. Expression of biglycan, decorin and proteoglycan-100/CSF-1 in normal and fibrotic human liver. Pathol Res Pract. 1997; 193:747–751. [PubMed: 9521506]
11. Ameye L, Aria D, Jepsen K, et al. Abnormal collagen fibrils in tendons of biglycan/fibromodulin-deficient mice lead to gait impairment, ectopic ossification, and osteoarthritis. FASEB J. 2002; 16:673–680. [PubMed: 11978731]
12. Hildebrand A, Romaris M, Rasmussen LM, et al. Interaction of the small interstitial proteoglycans biglycan, decorin and fibromodulin with transforming growth factor beta. Biochem J. 1994; 302:527–534. [PubMed: 8093006]
13. Hocking AM, Shinomura T, McQuillan DJ. Leucine-rich repeat glycoproteins of the extracellular matrix. Matrix Biol. 1998; 17:1–19. [PubMed: 9628249]
14. Svensson L, Aszodi A, Reinholt FP, et al. Fibromodulin-null mice have abnormal collagen fibrils, tissue organization, and altered lumican deposition in tendon. J Biol Chem. 1999; 274:9636–9647. [PubMed: 10092650]
15. Ezura Y, Chakravarti S, Oldberg A, et al. Differential expression of lumican and fibromodulin regulate collagen fibrillogenesis in developing mouse tendons. J Cell Biol. 2000; 151:779–788. [PubMed: 11076963]
16. Chakravarti S, Magnuson T, Lass JH, et al. Lumican regulates collagen fibril assembly: skin fragility and corneal opacity in the absence of lumican. J Cell Biol. 1998; 141:1277–1286. [PubMed: 9606218]
17. Grahame R. Joint hypermobility and genetic collagen disorders: are they related? Arch Dis Child. 1999; 80:188–191. [PubMed: 10325741]
18. Svensson L, Narlid I, Oldberg A. Fibromodulin and lumican bind to the same region on collagen type I fibrils. FEBS Lett. 2000; 470:178–182. [PubMed: 10734230]
19. Krull NB, Gressner AM. Differential expression of keratan sulphate proteoglycans fibromodulin, lumican and aggrecan in normal and fibrotic rat liver. FEBS Lett. 1992; 312:47–52. [PubMed: 1385211]
20. Goldberg M, Septier D, Oldberg A, et al. Fibromodulin-deficient mice display impaired collagen fibrillogenesis in predentin as well as altered dentin mineralization and enamel formation. J Histochem Cytochem. 2006; 54:525–537. [PubMed: 16344330]
21. Goldberg M, Ono M, Septier D, et al. Fibromodulin-deficient mice reveal dual functions for fibromodulin in regulating dental tissue and alveolar bone formation. Cells Tissues Organs. 2009; 189:198–202. [PubMed: 18698127]
22. Chakravarti S. Functions of lumican and fibromodulin: lessons from knockout mice. Glycoconj J. 2002; 19:287–293. [PubMed: 12975607]
23. Batts KP, Ludwig J. Chronic hepatitis. An update on terminology and reporting. Am J Surg Pathol. 1995; 19:1409–1417. [PubMed: 7503362]
24. Scheuer PJ. Classification of chronic viral hepatitis: a need for reassessment. J Hepatol. 1991; 13:372–374. [PubMed: 1808228]
25. Kleiner DE, Brunt EM, Van Natta M, et al. Design and validation of a histological scoring system for nonalcoholic fatty liver disease. Hepatology. 2005; 41:1313–1321. [PubMed: 15915461]
26. Bouchard G, Yousef IM, Barriault C, et al. Role of glutathione and oxidative stress in phalloidin-induced cholestasis. J Hepatol. 2000; 32:550–560. [PubMed: 10782902]
27. Urtasun R, Lopategi A, George J, et al. Osteopontin, an oxidant stress-sensitive cytokine, up-regulates collagen-i via integrin alpha(V) beta(3) engagement and PI3K-pAkt-NFkappaB signaling. Hepatology. 2011 Sep 27. [Epub ahead of print].
28. Greenwel P, Dominguez-Rosales JA, Mavi G, et al. Hydrogen peroxide: a link between acetaldehyde-elicited alpha1(I) collagen gene up-regulation and oxidative stress in mouse hepatic stellate cells. Hepatology. 2000; 31:109–116. [PubMed: 10613735]

29. Nieto N, Cederbaum AI. Increased Sp1-dependent transactivation of the LAMgamma 1 promoter in hepatic stellate cells co-cultured with HepG2 cells overexpressing cytochrome P450 2E1. J Biol Chem. 2003; 278:15360–15372. [PubMed: 12529372]

30. Nieto N, Friedman SL, Cederbaum AI. Cytochrome P450 2E1-derived reactive oxygen species mediate paracrine stimulation of collagen I protein synthesis by hepatic stellate cells. J Biol Chem. 2002; 277:9853–9864. [PubMed: 11782477]

31. Friedman SL, Wei S, Blaner WS. Retinol release by activated rat hepatic lipocytes: regulation by Kupffer cell-conditioned medium and PDGF. Am J Physiol. 1993; 264:G947–G952. [PubMed: 8498521]

32. Friedman SL, Arthur MJ. Activation of cultured rat hepatic lipocytes by Kupffer cell conditioned medium. Direct enhancement of matrix synthesis and stimulation of cell proliferation via induction of platelet-derived growth factor receptors. J Clin Invest. 1989; 84:1780–1785. [PubMed: 2556445]

33. Poole AR, Nelson F, Dahlberg L, et al. Proteolysis of the collagen fibril in osteoarthritis. Biochem Soc Symp. 2003; (70):115–123. [PubMed: 14587287]

34. Venkatesan N, Ebihara T, Roughley PJ, et al. Alterations in large and small proteoglycans in bleomycin-induced pulmonary fibrosis in rats. Am J Respir Crit Care Med. 2000; 161:2066–2073. [PubMed: 10852789]

35. Bevilacqua MA, Iovine B, Zambrano N, et al. Fibromodulin gene transcription is induced by ultraviolet irradiation, and its regulation is impaired in senescent human fibroblasts. J Biol Chem. 2005; 280:31809–31817. [PubMed: 16002407]

36. Iovine B, Nino M, Irace C, et al. Ultraviolet B and A irradiation induces fibromodulin expression in human fibroblasts in vitro. Biochimie. 2009; 91:364–372. [PubMed: 19041686]

37. Nieto N. Ethanol and fish oil induce NFkappaB transactivation of the collagen alpha2(I) promoter through lipid peroxidation-driven activation of the PKC-PI3K-Akt pathway. Hepatology. 2007; 45:1433–1445. [PubMed: 17538965]

38. Soo C, Hu FY, Zhang X, et al. Differential expression of fibromodulin, a transforming growth factor-beta modulator, in fetal skin development and scarless repair. Am J Pathol. 2000; 157:423–433. [PubMed: 10934147]

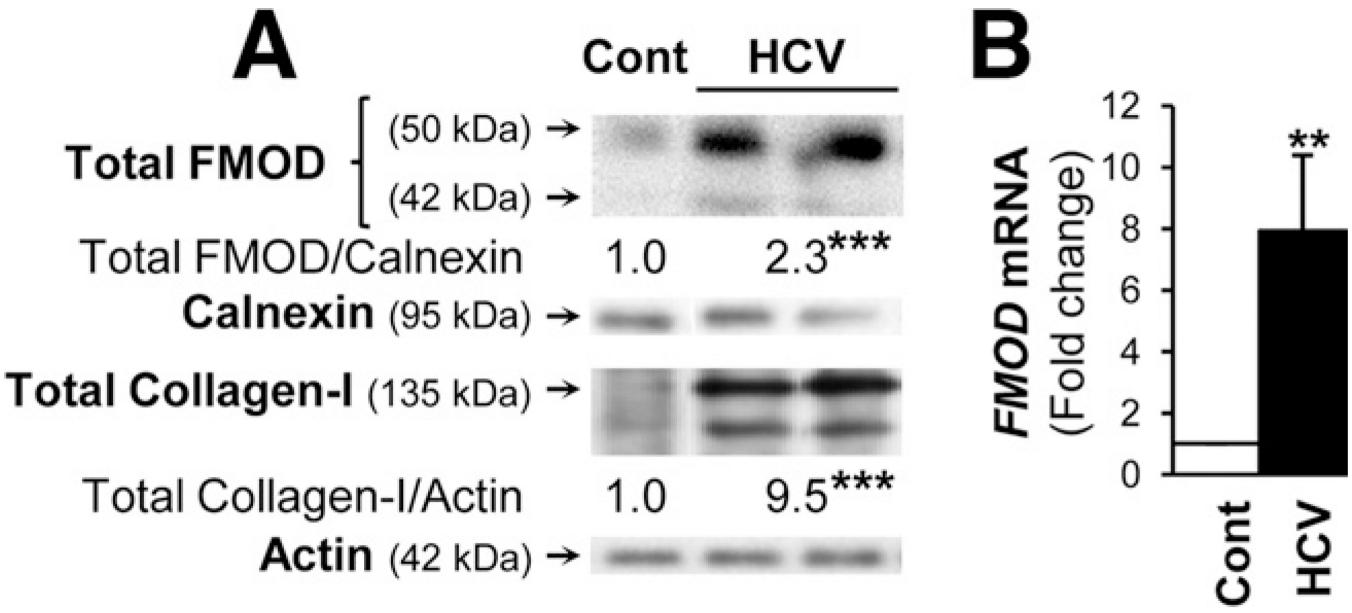

Figure 1.

FMOD expression increases in patients with HCV-induced cirrhosis. (*A*) Patients with biopsy-proven stage 3 HCV-induced cirrhosis showed an increase in FMOD and collagen I protein levels compared with healthy individuals. Likewise, there was a significant elevation in *FMOD* mRNA levels in patients with stage 3 HCV-induced cirrhosis compared with healthy liver explants. (*B*) The *bar graph* represents the fold change in *FMOD* mRNA normalized by that of *GAPDH*. n = 5; ** $P < .01$ and *** $P < .001$ for HCV-induced cirrhosis vs healthy explants.

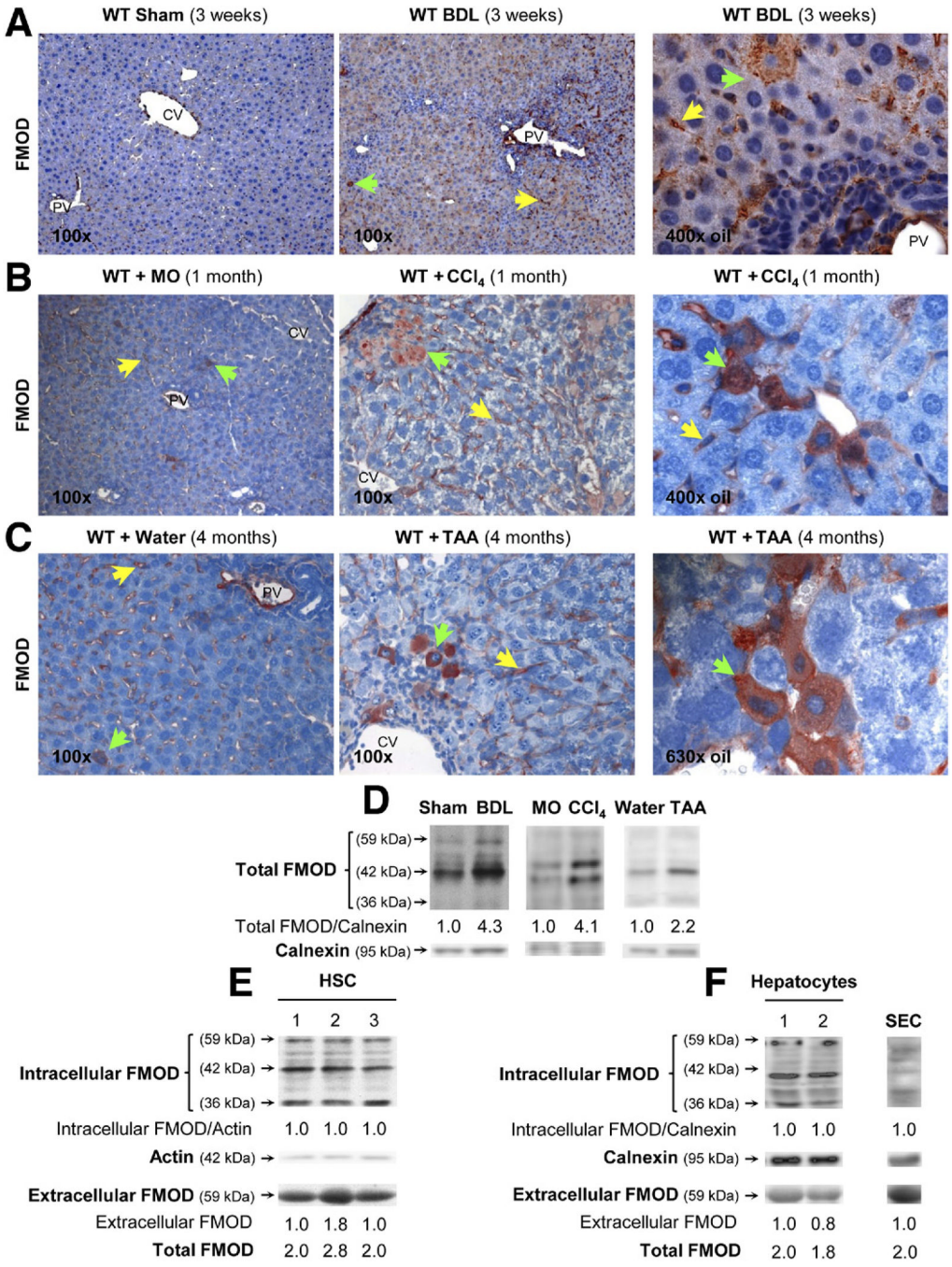

Figure 2.

FMOD expression is up-regulated in cholestasis and in drug-induced liver injury in mice. Ten-week-old male WT mice were (*A*) bile duct ligated for 3 weeks, (*B*) injected with CCl_4 for 1 month, or (*C*) treated with TAA for 4 months. IHC analysis depicted significant FMOD expression in all 3 models of liver injury in sinusoidal areas (*yellow arrows*) and in hepatocytes (*green arrows*). The pictures on the *right* show FMOD-positive staining at larger magnification (400×−630× oil). CV, central vein; PV, portal vein. (*D*) Total FMOD expression in the BDL, CCl_4, and TAA models evaluated by Western blot. Western blot analysis showing FMOD expression in independent isolations of (*E*) primary HSCs and (*F*)

hepatocytes and SECs from CCl_4-injured mice. The quantification of the intensity of the FMOD signal corrected by that of calnexin or actin is shown *under the blots*.

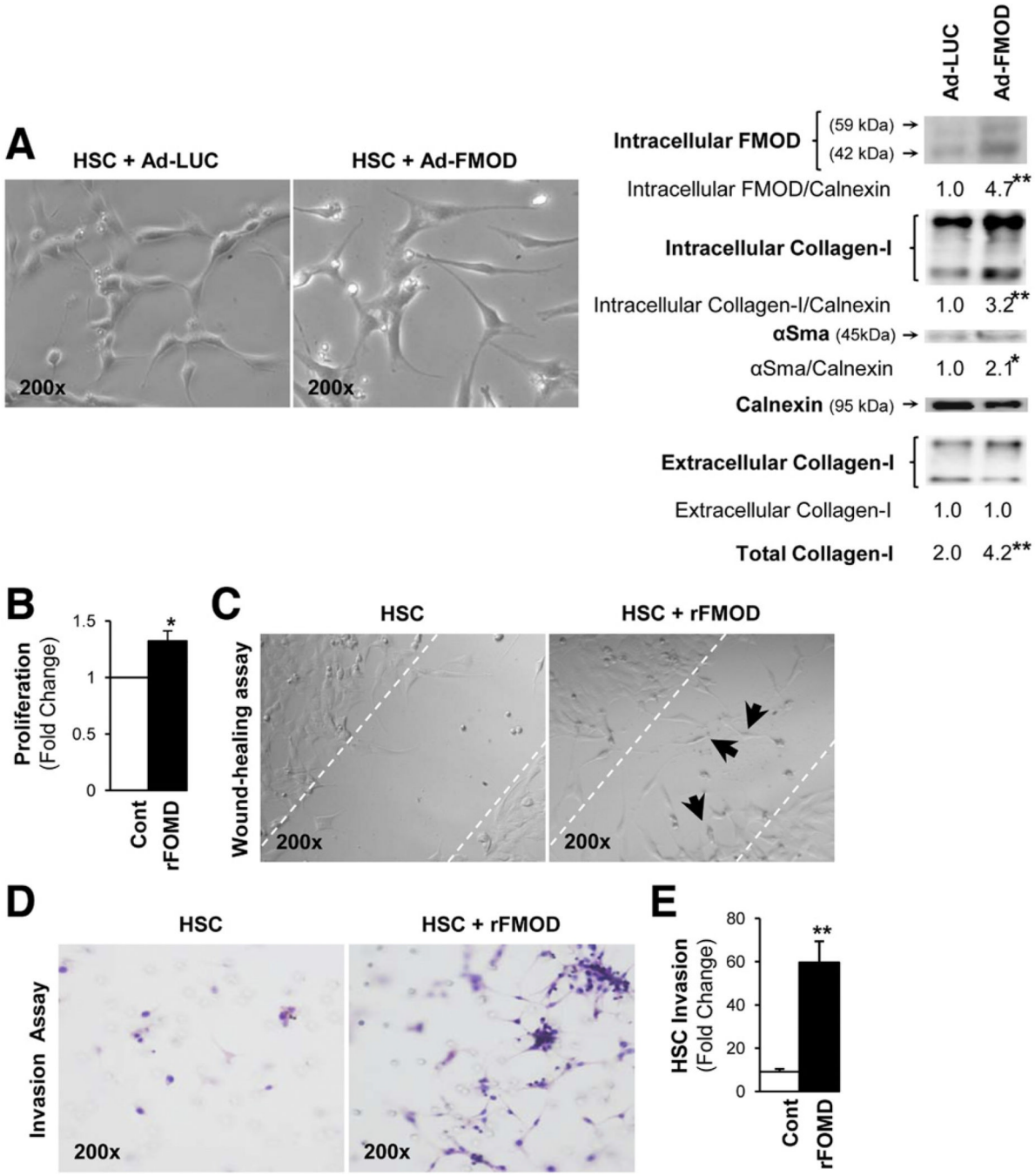

Figure 3.

FMOD activates and induces profibrogenic effects in HSCs. Rat HSCs from fewer than 3 passages were (*A*) infected with Ad-LUC or Ad-FMOD or (*B–E*) were treated with rFMOD. (*A, left*) Light micrographs showing similar HSC viability and absence of phenotypic changes under adenoviral infection. (*A, right*) Western blot analysis proved efficient intracellular FMOD expression in Ad-FMOD–infected HSCs, which was associated with an increase in collagen I and α-SMA expression. Treatment with rFMOD enhanced (*B*) HSC proliferation, (*C*) migration in the wound-healing assay (*arrows* showing the migratory cells), and (*D* and *E*) invasion or chemotaxis. Results are expressed as average values.

Experiments were performed in triplicate 4 times; *$P < .05$ and **$P < .01$ for Ad-FMOD or rFMOD vs Ad-LUC or control.

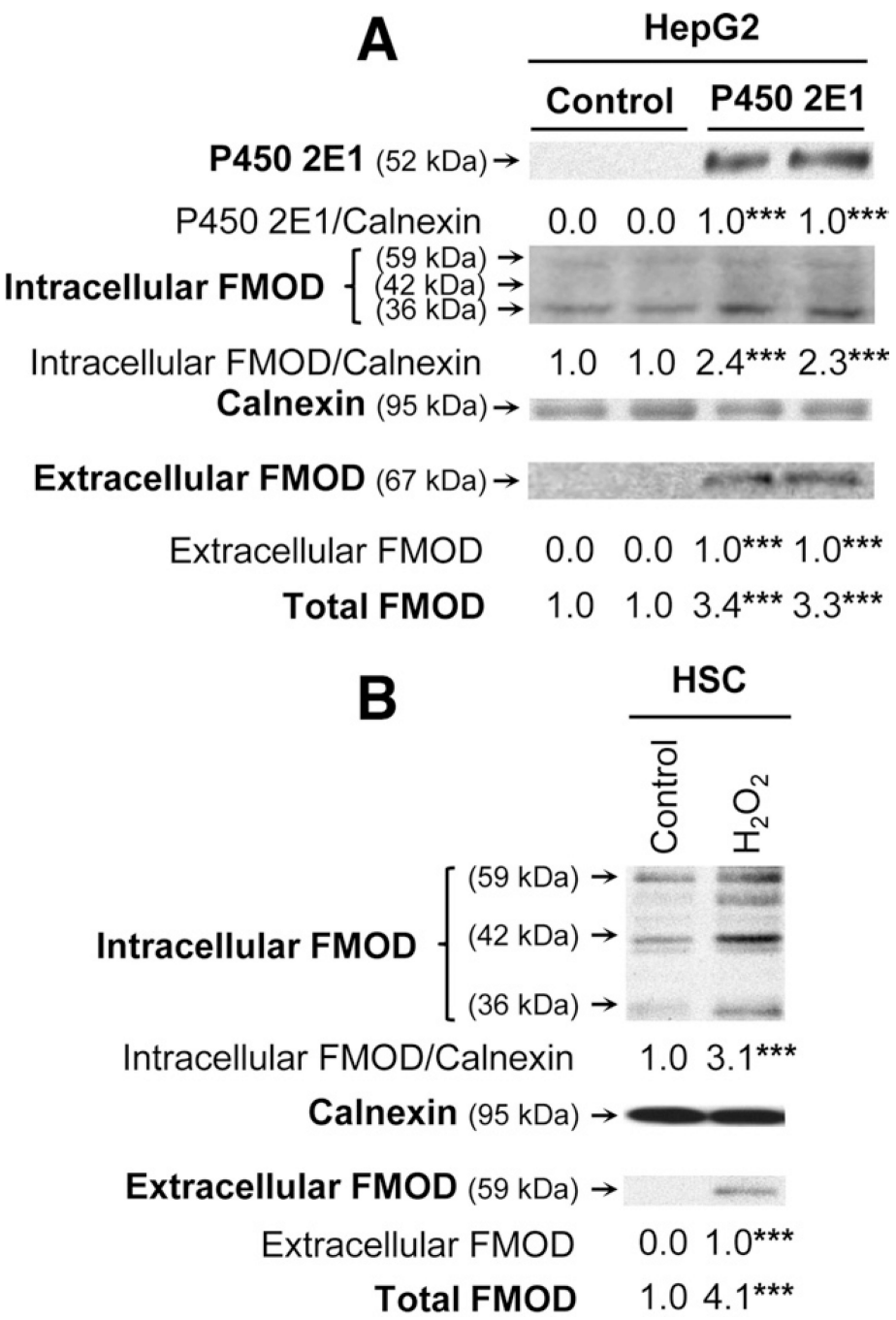

Figure 4.

ROS increase FMOD protein expression. (*A*) Western blot analysis for intracellular and extracellular FMOD protein induction in a stable HepG2 cell line transduced to overexpress cytochrome P450 2E1 as a source of ROS. (*B*) Primary rat HSCs incubated with H_2O_2 showed greater intracellular and extracellular FMOD protein expression than non-treated HSCs. Results are expressed as average values. Experiments were performed in triplicate 4 times. ***$P < .001$ for P450 2E1 or H_2O_2-treated vs control.

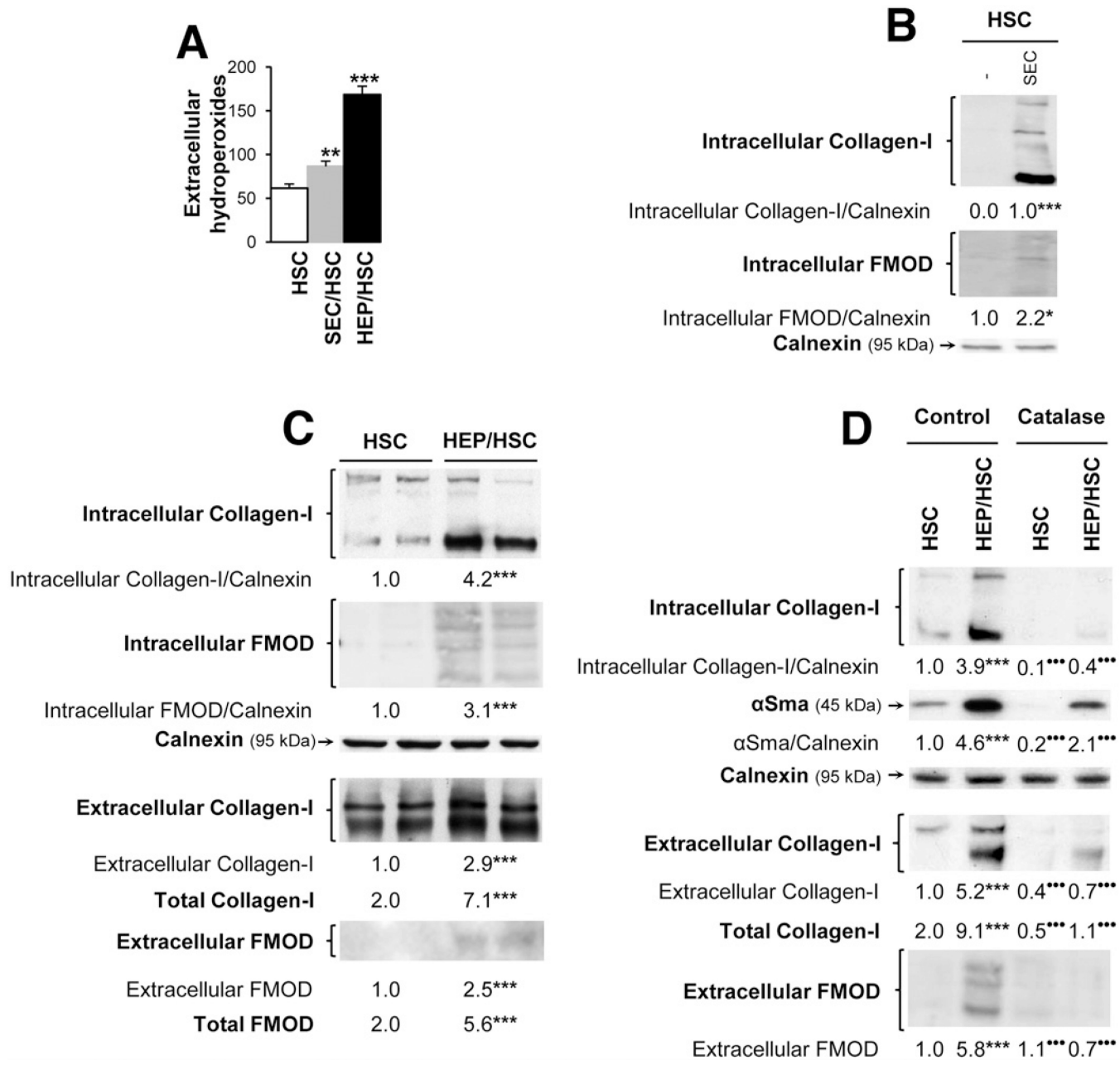

Figure 5.

Coculture with hepatocytes or SECs increases ROS and FMOD and collagen I level in HSCs. Primary rat HSCs cultured for 3 days were placed in coculture with either primary SECs or hepatocytes, and cell lysates and culture medium were collected 24 hours later. (*A*) ROS (mostly hydroperoxides) in the cell culture medium. Intracellular FMOD and collagen I expression in the HSC and SEC coculture and HSC monoculture. (*B*) Extracellular proteins were undetectable. (*C*) Intracellular and extracellular collagen I and FMOD expression in the HSC and hepatocyte coculture and HSC monoculture. (*D*) Catalase blocked the effect of the cocultures on FMOD, collagen I, and α-SMA. Results are expressed as average values. Experiments were performed in triplicate 4 times. **P* < .05, ***P* < .01, and ****P* < .001 for coculture vs monoculture; •••*P* < .001 for catalase vs control.

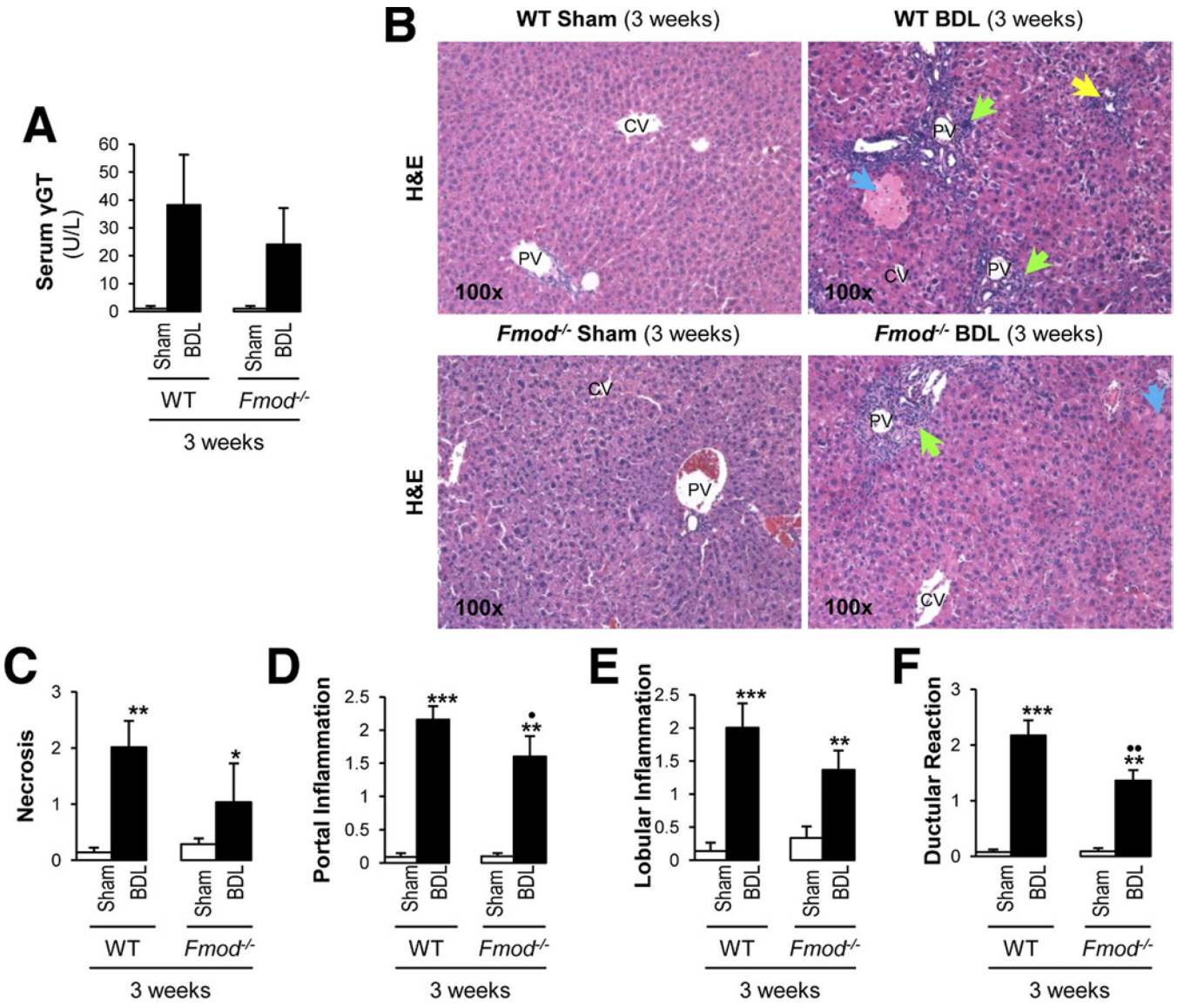

Figure 6.

WT mice show more BDL-induced liver injury than *Fmod*$^{-/-}$ mice. Ten-week-old male WT and *Fmod*$^{-/-}$ mice were subjected to common BDL or sham operation and were killed 3 weeks later. The activity of γ-glutamyltransferase is shown in *panel A*. (*B*) H&E staining demonstrating greater necrosis (*blue arrows*), inflammation (*yellow arrow*), and ductular reaction (*green arrows*) in BDL WT than in *Fmod*$^{-/-}$ mice. The Brunt pathology scores for necrosis, portal inflammation, lobular inflammation, and ductular reaction are shown in *panels C* to *F*. CV, central vein; PV, portal vein. n = 6/group; **P* < .05, ***P* < .01, and ****P* < .001 for BDL vs sham; •*P* < .05 and ••*P* < .01 for BDL *Fmod*$^{-/-}$ vs BDL WT.

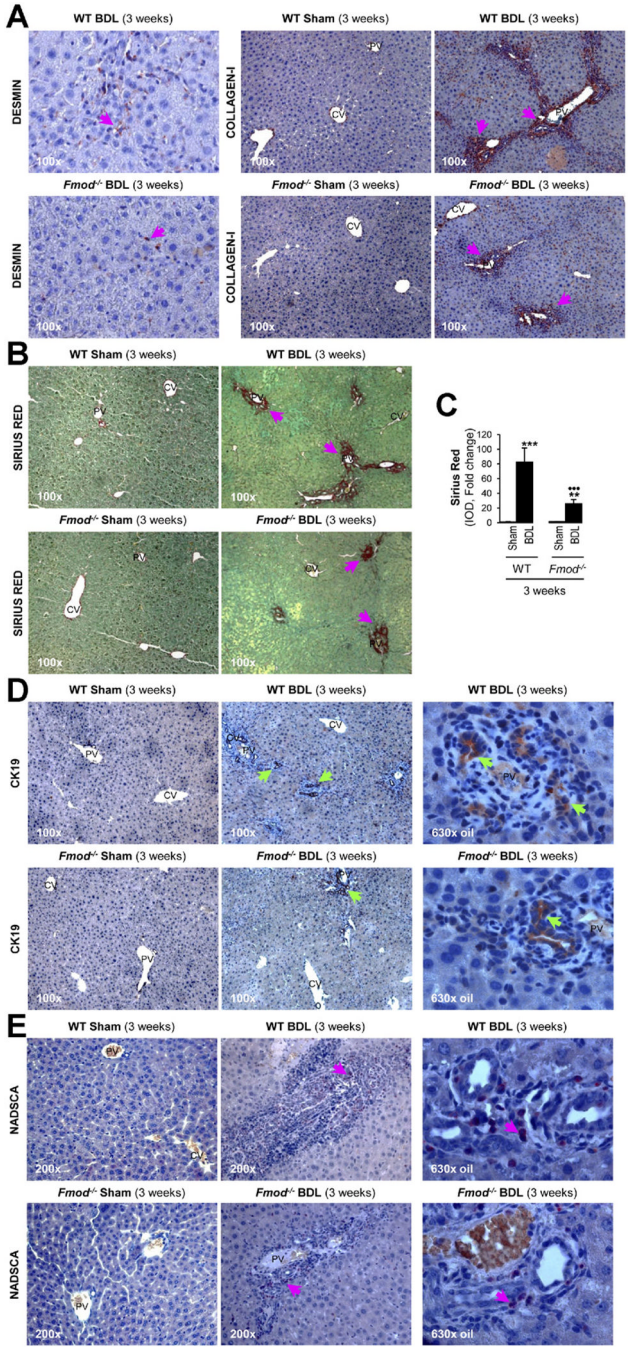

Figure 7.

WT mice show more BDL-induced fibrosis, ductular reaction, and neutrophil infiltration than *Fmod*$^{-/-}$ mice. (*A*) IHC depicted more desmin and collagen I protein in BDL WT mice than in *Fmod*$^{-/-}$ mice (*pink arrows*). (*B* and *C*) Sirius red/fast green staining and morphometry (*pink arrows*). (*D*) IHC for cytokeratin-19 (*green arrows*). (*E*) Naphthol AS-D Chloroacetate Esterase (NADSCA) staining to demonstrate the presence of neutrophils (*pink arrows*). CV, central vein; PV, portal vein. n = 6/group. Results are expressed as average values. $^{**}P < .01$ and $^{***}P < .001$ for BDL vs sham and $^{\bullet\bullet\bullet}P < .001$ for *Fmod*$^{-/-}$ vs WT.